

# Optimizing the performance of the near-infrared (NIR) photothermal conversion via modulating the domain size of chiral nematic phase in the co-assembled cellulose nanocrystals composite films

Kai Feng, Guodan Wei, Mengfan Lu, Naiwei Gao, Yapei Wang and Zhaoxia Jin\*

Key Laboratory of Advanced Light Conversion Materials and Biophotonics,  
Department of Chemistry, Renmin University of China, 100872 Beijing, People's  
Republic of China

\*Email: jinzx@ruc.edu.cn

## Content

### Figures

<b>Fig. S1</b> The vis-NIR transmittance spectra (a) and CD spectra (b) of pure CNCs and CP <sub>x</sub> composite films.....	S4
<b>Fig. S2</b> Cross-sectional SEM images of (a) CP <sub>1</sub> ; (b) CP <sub>2</sub> ; (c) CP <sub>3</sub> ; (d) CP <sub>4</sub> , (e) CP <sub>5</sub> and (f) CP <sub>6</sub> composite film.....	S5
<b>Fig. S3</b> The magnified cross-sectional SEM images of (a) CP <sub>5</sub> and (b) CP <sub>6</sub> compositefilm.....	S6
<b>Fig. S4</b> UV-vis-NIR absorption spectrum of pure PEDOT: PSS film.....	S7
<b>Fig. S5</b> The surface temperature of CP <sub>x</sub> composite films induced by NIR light irradiation (750 nm) under different power.....	S8
<b>Fig. S6</b> The surface temperature of CP <sub>x</sub> film increases and decreases through alternatively turn-on and turn-off light irradiation under different power. (a) CP <sub>1</sub> ; (b)	

CP<sub>2</sub>; (c) CP<sub>3</sub>; (d) CP<sub>4</sub>; (e) CP<sub>5</sub>; (f) CP<sub>6</sub> composite film.....S9

**Fig. S7** A linear fitting correlation between cooling period ( $t$ ) and  $-\ln\theta$  with an  $R$ -squared value of over 0.99.  $\theta$  refers to the ratio of  $\Delta T$  to  $\Delta T_{max}$ .....S10

**Fig. S8** The cross-sectional SEM image of (a) HPC/PEDOT: PSS/OS/TA with 3.43 wt.% PEDOT; (c) PVP/PEDOT: PSS/OS/TA with 3.43 wt.% PEDOT; POM image of (b) HPC/PEDOT: PSS/OS/TA with 3.43 wt.% PEDOT; (d) PVP/PEDOT: PSS/OS/TA with 3.43 wt.% PEDOT.....S11

**Fig. S9** The increase and decrease of the surface temperature of pure PEDOT: PSS film through alternative turn-on and turn-off light irradiation under different power.....S1

2

**Fig. S10** POM images of (a) CNCs/PEDOT: PSS/OS and (b) CNCs/PEDOT: PSS/TA film.....S13

**Fig. S11** POM image of pure CNCs film.....S14

**Fig. S12** POM image of CP<sub>6</sub> composite film.....S15

**Fig. S13** POM images of CNCs/PEDOT: PSS composite films with the mass ratio of (a) CNCs : (PEDOT: PSS) = 95:5; (b) CNCs : (PEDOT: PSS) = 80:20.....S16

**Fig. S14** (a) POM image of pure CNCs (b.d.) film. (b) The cross-sectional SEM image of pure CNCs (b.d.) film.....S17

**Fig. S15** The comparison of temperature changes of CP<sub>x</sub> composite films (the red line) and CP<sub>x</sub> (b.d.) films (the black line) with different PEDOT: PSS contents, under the 1.5 W light radiation (750 nm laser).....S18

## Tables

**Table S1** Sample codes of CP<sub>x</sub> composite films.....S19

**Table S2** The compositions of CNCs/PEDOT: PSS, CNCs/PEDOT: PSS/OS, CNCs/PEDOT: PSS/TA, PEDOT: PSS/OS/TA, HPC/PEDOT: PSS/OS/TA, PVP/PEDOT: PSS/OS/TA, and CNCs(b.d.)/PEDOT: PSS/OS/TA composite films.....S20

**Table S3** NIR photothermal conversion efficiency ( $\eta_{PT}$ ) of pure PEDOT: PSS and CP<sub>x</sub> composite films.....S22

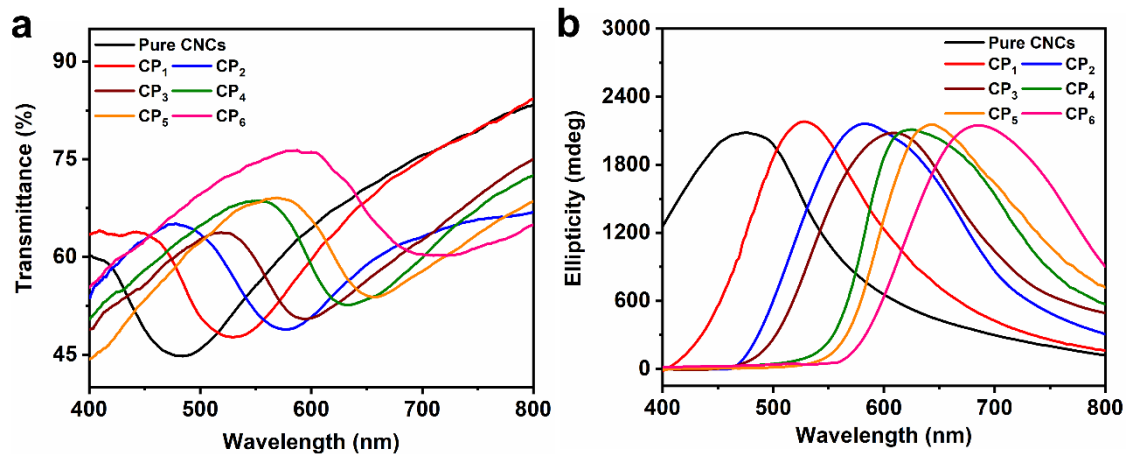


**Fig. S1** The vis-NIR transmittance spectra (a) and CD spectra (b) of pure CNCs and CP<sub>x</sub> composite films.

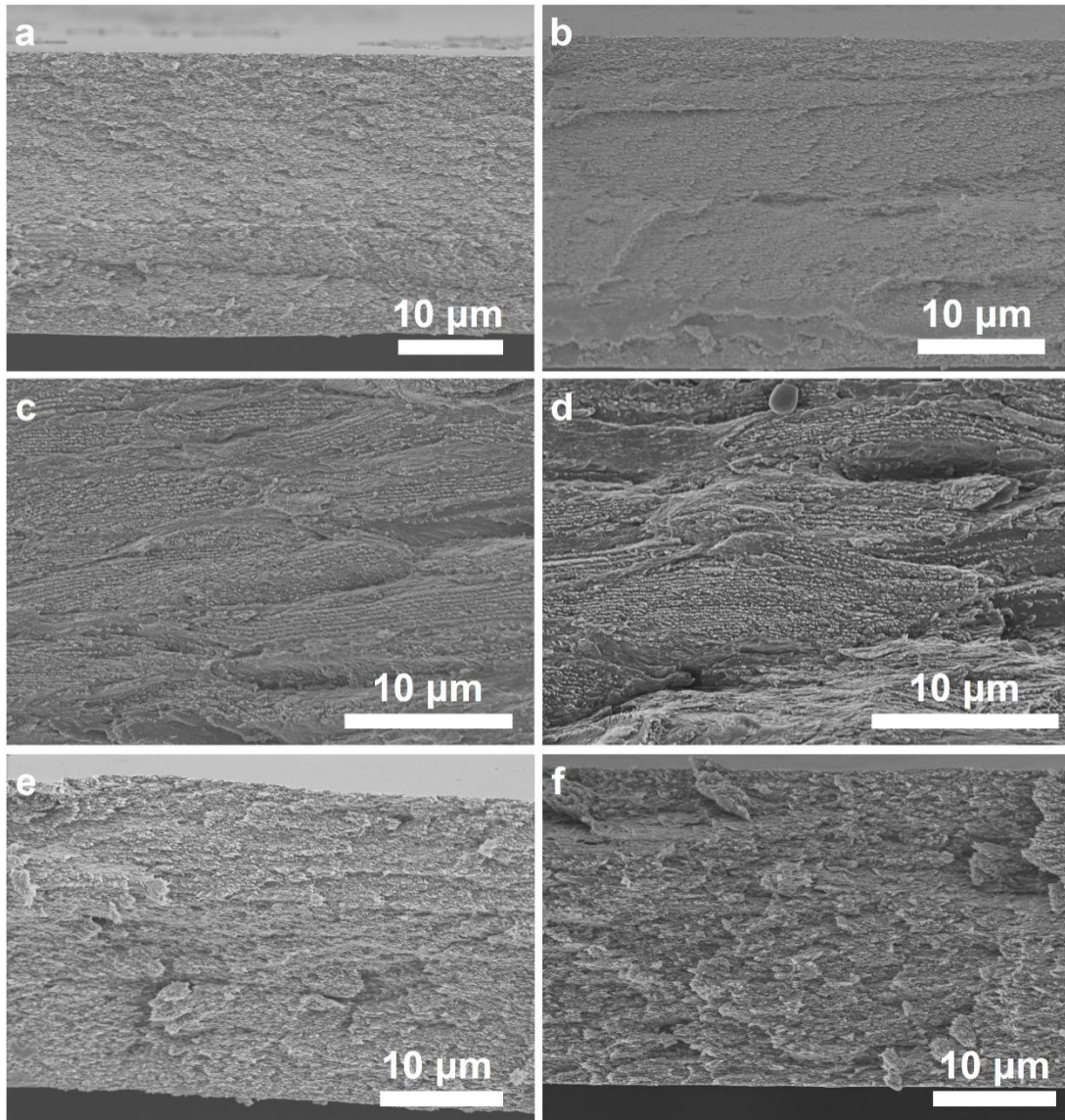


**Fig. S2** Cross-sectional SEM images of (a) CP<sub>1</sub>; (b) CP<sub>2</sub>; (c) CP<sub>3</sub>; (d) CP<sub>4</sub>, (e) CP<sub>5</sub> and (f) CP<sub>6</sub> composite film.

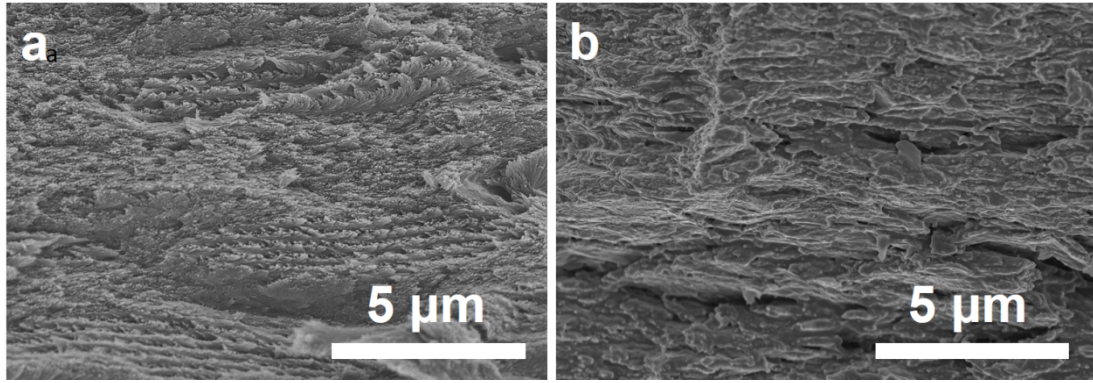


**Fig. S3** The magnified cross-sectional SEM images of (a) CP<sub>5</sub> and (b) CP<sub>6</sub> composite film.

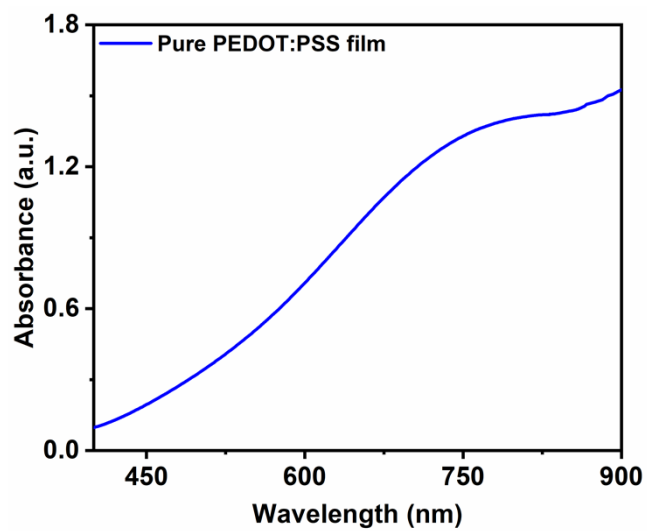


**Fig. S4** UV-vis-NIR absorption spectrum of pure PEDOT: PSS film.

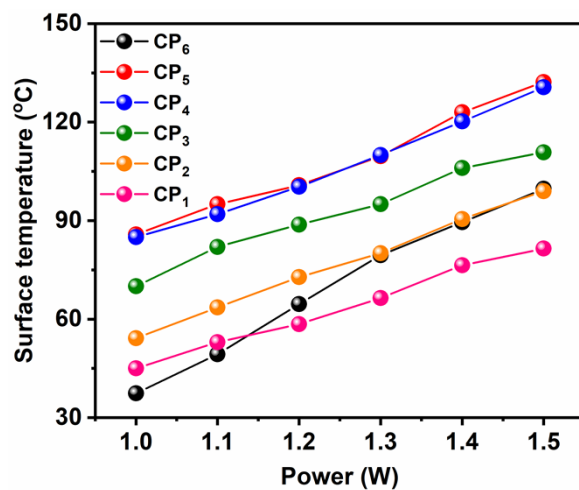


**Fig. S5** The surface temperature of CP<sub>x</sub> composite films induced by NIR light irradiation (750 nm) under different power of light.



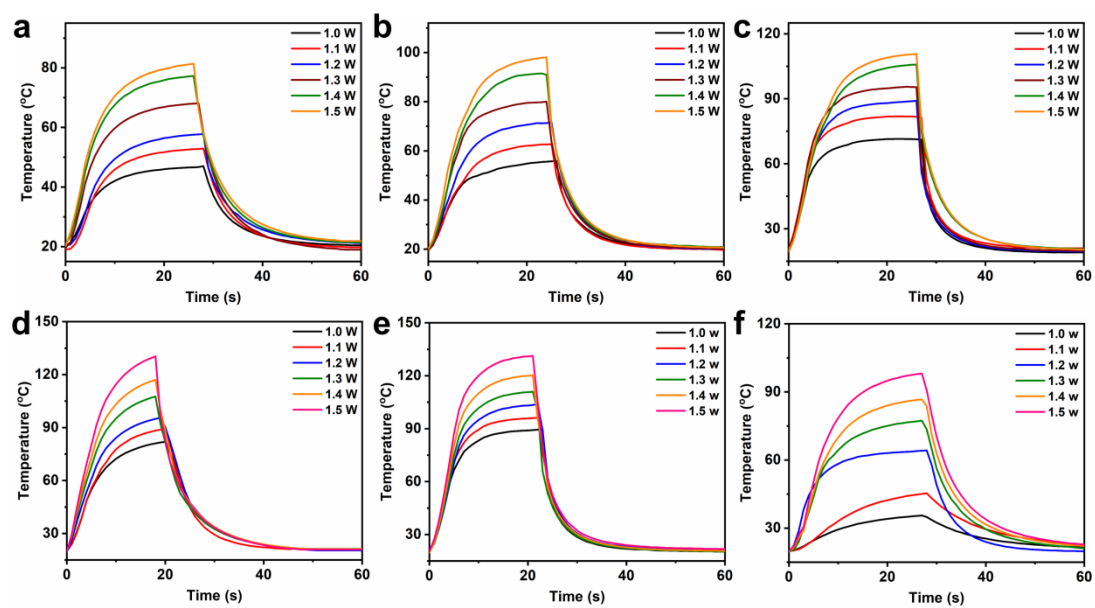


**Fig. S6** The surface temperature of CP<sub>x</sub> film increases and decreases through alternatively turn-on and turn-off light irradiation under different power. (a) CP<sub>1</sub>; (b) CP<sub>2</sub>; (c) CP<sub>3</sub>; (d) CP<sub>4</sub>; (e) CP<sub>5</sub>; (f) CP<sub>6</sub> composite film.

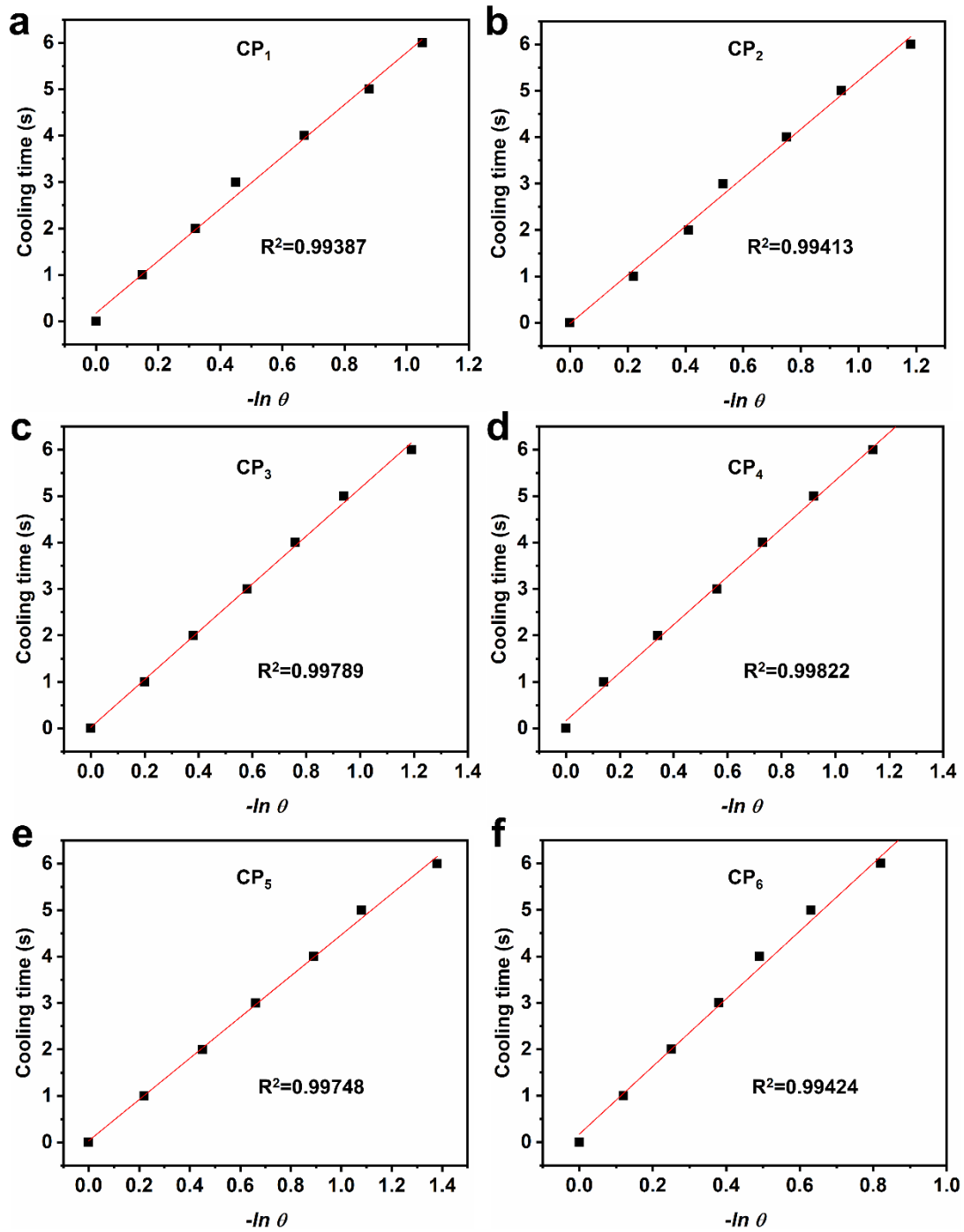


**Fig. S7** A linear fitting correlation between cooling period ( $t$ ) and  $-\ln \theta$  with an  $R$ -squared value of over 0.99.  $\theta$  refers to the ratio of  $\Delta T$  to  $\Delta T_{max}$ .

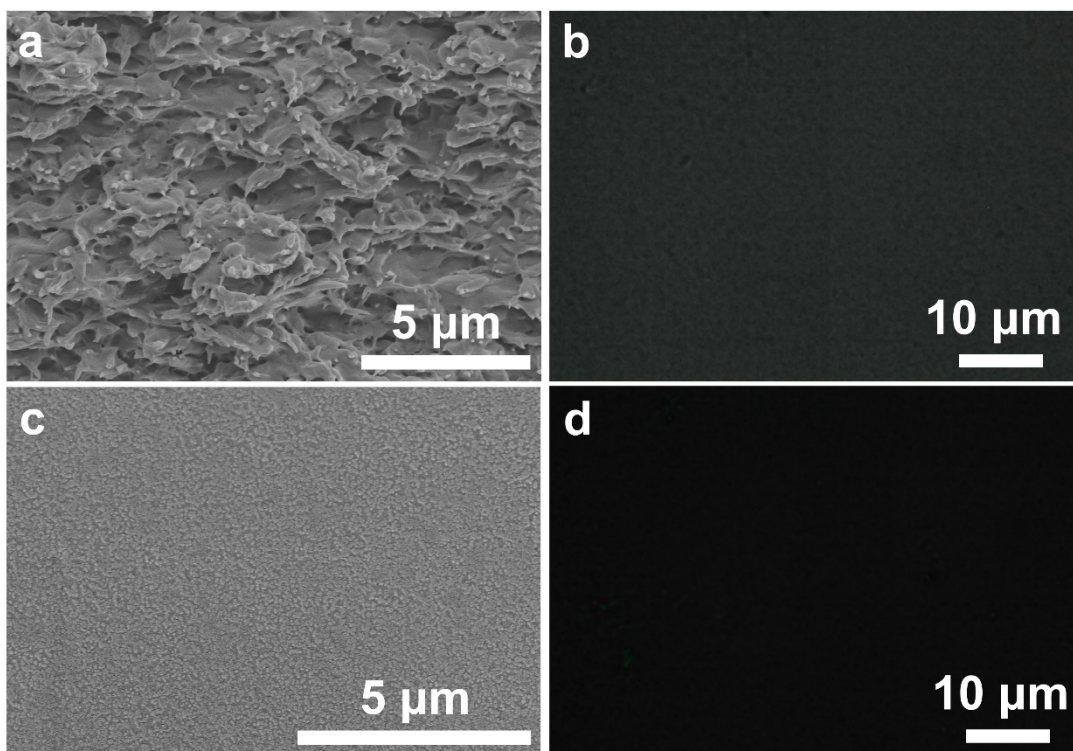


**Fig. S8** Characterizations of HPC/PEDOT: PSS/OS/TA (a, b) and PVP/PEDOT: PSS/OS/TA (c, d). Both samples contained 3.43 wt.% PEDOT. (a, c) The cross-sectional SEM images. (b, d) POM images. These images confirmed that there was no chiral nematic nanostructure in these composite films.

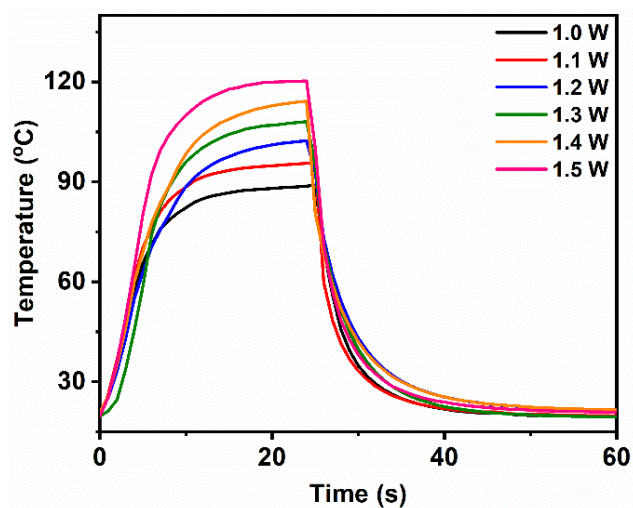


**Fig. S9** The increase and decrease of the surface temperature of pure PEDOT: PSS film through alternative turn-on and turn-off light irradiation under different power.

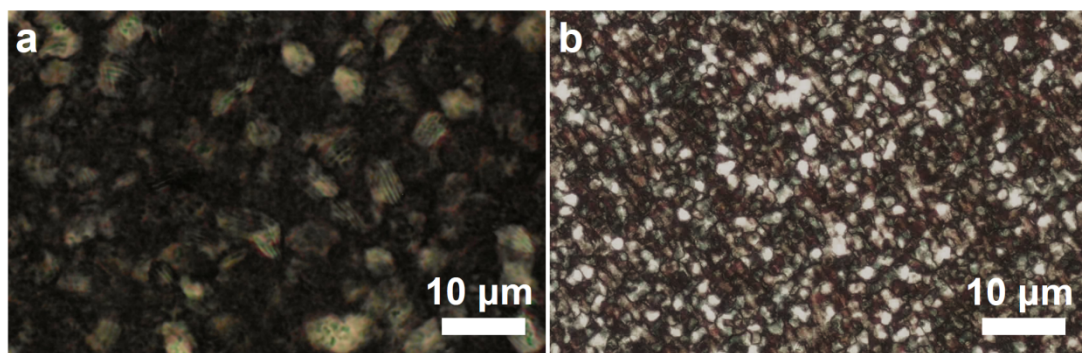


**Fig. S10** POM images of (a) CNCs/PEDOT: PSS/OS and (b) CNCs/PEDOT: PSS/TA film.

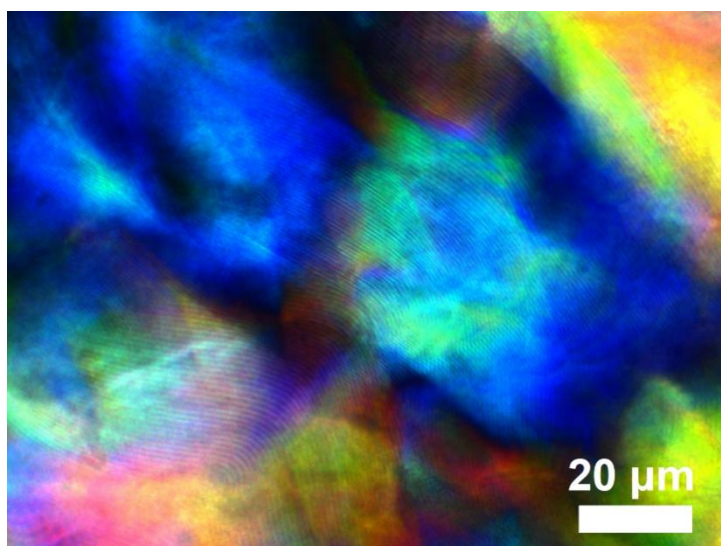


**Fig. S11** POM image of pure CNCs film.

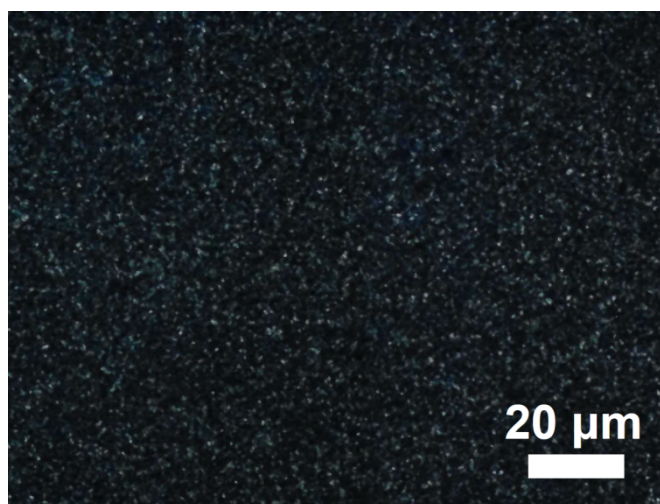


**Fig. S12** POM image of CP<sub>6</sub> composite film.

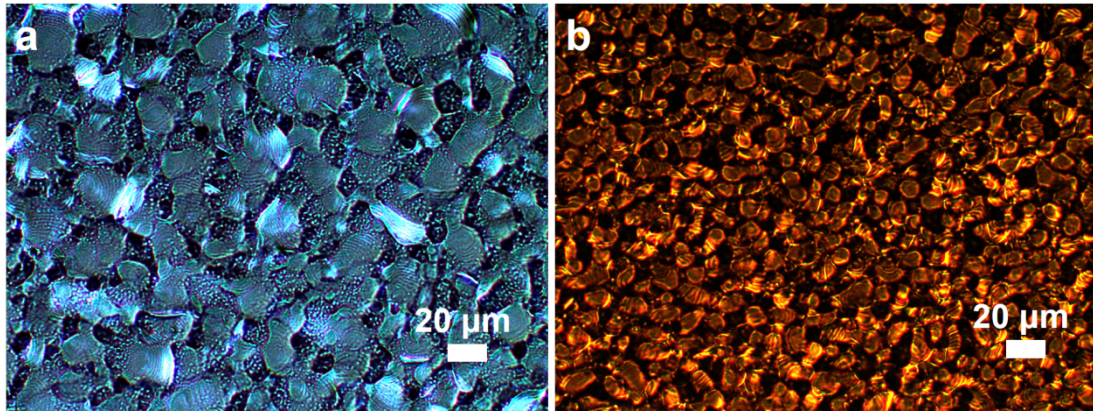


**Fig. S13** POM images of CNCs/PEDOT: PSS composite films with the mass ratio of (a) CNCs : (PEDOT: PSS) = 95:5; (b) CNCs : (PEDOT: PSS) = 80:20.



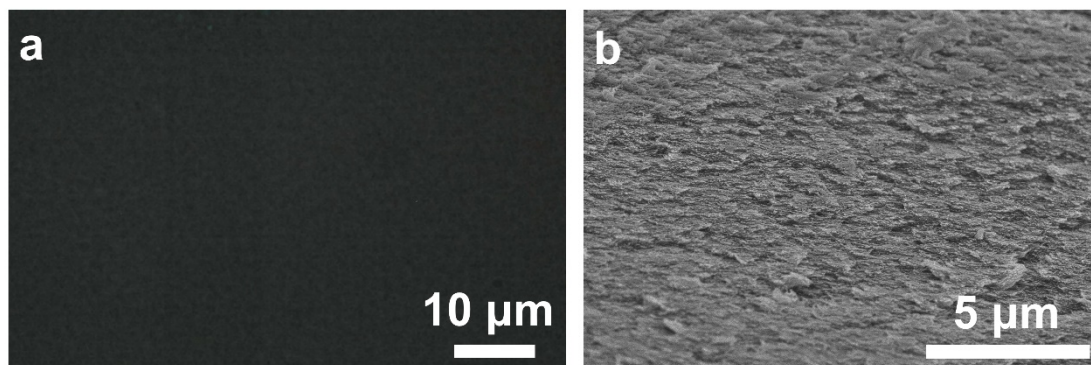


**Fig. S14** (a) POM image of pure CNCs (b.d.) film. (b) The cross-sectional SEM image of pure CNCs (b.d.) film.

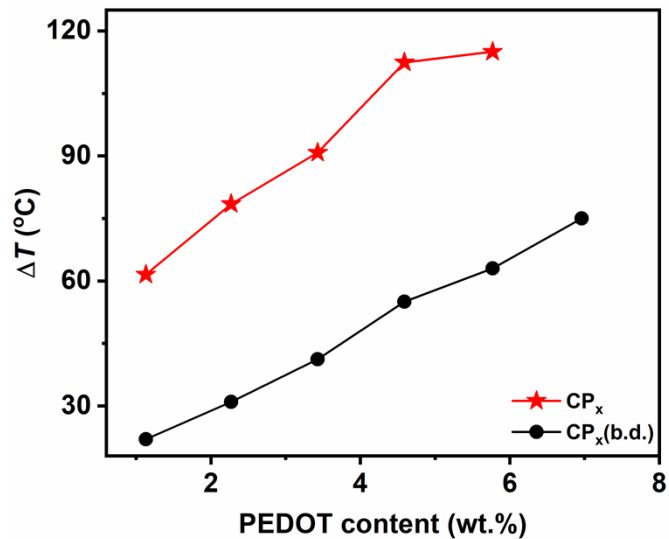


**Fig. S15** The comparison of temperature changes of  $CP_x$  composite films (the red line) and  $CP_x$  (b.d.) films (the black line) with different PEDOT: PSS contents, under the 1.5 W light radiation (750 nm laser).

**Table S1** Sample codes of CP<sub>x</sub> composite films.

Sample codes	Weight ratio
	CNCs : (PEDOT:PSS) : OS : (TA + zonyl) <sup>a</sup>
CP <sub>1</sub>	75.19 : 3.96 : 8.35 : 12.50
CP <sub>2</sub>	71.60 : 7.95 : 7.95 : 12.50
CP <sub>3</sub>	67.96 : 11.99 : 7.55 : 12.50
CP <sub>4</sub>	64.29 : 16.07 : 7.14 : 12.50
CP <sub>5</sub>	60.58 : 20.19 : 6.73 : 12.50
CP <sub>6</sub>	56.83 : 24.36 : 6.31 : 12.50

<sup>a</sup> The ratios of TA and zonyl were kept at 10 % and 2.5 %, respectively.

**Table S2** The compositions of CNCs/PEDOT: PSS, CNCs/PEDOT: PSS/OS, CNCs/PEDOT: PSS/TA, PEDOT: PSS/OS/TA, HPC/PEDOT: PSS/OS/TA, PVP/PEDOT: PSS/OS/TA and CNCs(b.d.)/PEDOT: PSS/OS/TA composite films.

Sample	Weight ratio
CNCs/PEDOT: PSS	CNCs : (PEDOT: PSS)
	93.54 : 3.96
	89.55 : 7.95
	85.51 : 11.99
	81.43 : 16.07
	77.31 : 20.19
CNCs/PEDOT: PSS/OS	CNCs : (PEDOT: PSS) : OS <sup>a</sup>
	84.19 : 3.96 : 9.35
	80.60 : 7.95 : 8.95
	76.96 : 11.99 : 8.55
	73.29 : 16.07 : 8.14
	69.58 : 20.19 : 7.73
CNCs/PEDOT: PSS/TA	CNCs : (PEDOT: PSS) : TA <sup>a</sup>
	83.54 : 3.96 : 10
	79.55 : 7.95 : 10
	75.51 : 11.99 : 10

	71.43 : 16.07 : 10
	67.31 : 20.19 : 10
PEDOT: PSS/OS/TA	(PEDOT: PSS) : OS : TA : Zonyl
	15.96 : 33.66 : 40.31 : 10.07
	27.99 : 27.99 : 35.21 : 8.81
	37.42 : 23.56 : 31.21 : 7.81
	45.00 : 19.99 : 28.00 : 7.01
	51.22 : 17.07 : 25.37 : 6.34
HPC (or PVP, CNCs(b.d))/PEDOT: PSS/OS/TA	HPC (or PVP, CNC(b.d)) : (PEDOT: PSS) : OS :
	TA <sup>a</sup>
	75.19 : 3.96 : 8.35 : 10
	71.60 : 7.95 : 7.95 : 10
	67.96 : 11.99 : 7.55 : 10
	64.29 : 16.07 : 7.14 : 10
	60.58 : 20.19 : 6.73 : 10

<sup>a</sup>: The zonyl content was kept at 2.5% if not specified.

**Table S3** NIR photothermal conversion efficiency ( $\eta_{PT}$ ) of pure PEDOT: PSS and CP<sub>x</sub> composite films.

Samples	PEDOT content (wt.%)	$\eta_{PT}$ (%)
(Pure PEDOT: PSS)	28.57	68.7
CP <sub>1</sub>	1.13	71.2
CP <sub>2</sub>	2.27	73.8
CP <sub>3</sub>	3.43	77.0
CP <sub>4</sub>	4.59	77.0
CP <sub>5</sub>	5.77	77.6
CP <sub>6</sub>	6.96	64.2